

Adapted numerical methods for advection-reaction-diffusion problems generating periodic wavefronts

Raffaele D'Ambrosio, Martina Moccaldi, Beatrice Paternoster

*Department of Mathematics, University of Salerno, Fisciano (Sa), Italy
e-mail: rdambrosio@unisa.it, mmoccaldi@unisa.it, beapat@unisa.it*

Abstract

The paper presents an adapted numerical integration for advection-reaction-diffusion problems. The numerical scheme, exploiting the a-priori knowledge of the qualitative behaviour of the solution, gains advantages in terms of efficiency and accuracy with respect to classic schemes already known in literature. The adaptation is here carried out through the so-called trigonometrical fitting technique for the discretization in space, giving rise to a system of ODEs whose vector field contains both stiff and non-stiff terms. Due to this mixed nature of the vector field, an Implicit-Explicit (IMEX) method is here employed for the integration in time, based on the first order forward-backward Euler method. The coefficients of the method here introduced rely on unknown parameters which have to be properly estimated. In this work, such an estimate is performed by minimizing the leading term of the local truncation error. The effectiveness of this problem-oriented approach is shown through a rigorous theoretical analysis and some numerical experiments.

Keywords: Advection-reaction-diffusion problems, periodic plane wave solutions, trigonometrical fitting, parameter estimation, adapted method of lines, IMEX methods.

1. Introduction

The treatise is devoted to the numerical integration of nonlinear advection-reaction-diffusion problems having periodic waves as fundamental solutions. The general expression of such systems is the following:

$$\begin{aligned}\frac{\partial u}{\partial t} &= d_1 \frac{\partial^2 u}{\partial x^2} + a_1 \frac{\partial u}{\partial x} + f_1(u, v), \\ \frac{\partial v}{\partial t} &= d_2 \frac{\partial^2 v}{\partial x^2} + a_2 \frac{\partial v}{\partial x} + f_2(u, v),\end{aligned}\tag{1.1}$$

with proper initial and boundary conditions. The functions $u, v : \mathcal{D} = [0, X] \times [0, \infty) \rightarrow \mathbb{R}$ are state variables denoting, for example, the concentrations of certain

interacting biological species; the advection coefficients a_1 and a_2 represent the velocities of the transport medium, such as water or air; the terms $d_1 > 0$ and $d_2 > 0$ are diffusion coefficients and may also include the parametrizations of turbulence. The reaction term $[f_1(u, v), f_2(u, v)]^T$ is linked to the interactions between the various involved species and generally models the results of their chemical interactions. These systems are widely used in the applications: for instance, they are employed to model air pollution phenomena [16] or to understand morphogenesis [18].

For the numerical integration of such problems, classic methods could require a very small step-size to accurately follow the oscillatory behaviour of the exact solution because they are based on general purpose formulae constructed in order to be exact (within round-off error) on polynomials up to a certain degree. Since we focus on systems having an oscillating exact solution, it may be more convenient to employ fitted formulae developed in order to be exact on functions other than polynomials: this strategy is nowadays well-known as *trigonometrical fitting* (see [14, 17] and references therein) and the basis functions are typically supposed to belong to a finite-dimensional space called fitting space. The choice of a suitable fitting space is suggested by the a-priori known information about the exact solution, so the coefficients of the resulting adapted method are no longer constant as in the classic case, but rely on a parameter characterizing the exact solution, whose value is clearly unknown. As a result, the trigonometrical fitting strategy implies two main challenges: the choice of a suitable fitting space and the accurate estimate of the unknown parameters. In this paper, the oscillatory dynamics of the considered problems suggests the adoption of a trigonometrically fitted space and the minimization of the leading term of the local truncation error allows to accurately estimate the parameter.

Extending the ideas introduced in [6], we present a numerical scheme which spatially discretizes the system (1.1) by means of trigonometrically fitted finite differences and employs an Implicit-Explicit (IMEX) method, based on the first order forward-backward Euler method, to integrate in time the resulting system of ordinary differential equations

$$y' = Ay + f(y),$$

where A is a matrix whose size depends on the number of spatial grid points and $f(y)$ is a vector-valued function.

The choice of a time integration scheme based on IMEX method is suggested by the mixture nature of such system actually composed by stiff components (arising from the diffusion term) and nonlinear ones (coming from the reaction and the advection terms). Indeed, an IMEX numerical method implicitly integrates the stiff terms and explicitly integrates the others [2, 19, 30], obtaining benefits in term of efficiency and stability.

The paper is organized as follows: in Section 2 and 3 we develop a problem-oriented numerical scheme for the general advection-reaction-diffusion system (1.1); Section 4 concerns the rigorous analysis of accuracy and stability properties of the introduced method and the estimate of the parameters appearing in the coefficients of the method, while Section 5 provides some numerical experiments. Finally, Section 6 is devoted to present some conclusions.

2. An adapted numerical scheme

We aim to solve system (1.1), equipped by the following initial conditions

$$u(x, 0) = \psi_1(x), \quad v(x, 0) = \psi_2(x), \quad x \in [0, X], \quad (2.1)$$

and periodic boundary conditions

$$\begin{aligned} u(0, t) &= u(X, t), & v(0, t) &= v(X, t), \\ \frac{\partial u}{\partial t}(0, t) &= \frac{\partial u}{\partial t}(X, t), & \frac{\partial v}{\partial t}(0, t) &= \frac{\partial v}{\partial t}(X, t). \end{aligned} \quad (2.2)$$

Following the method of lines (see [13, 20, 21] and references therein), we spatially discretize the domain \mathcal{D} in

$$\mathcal{D}_h = \{(x_i, t) : x_i = ih, i = 0, \dots, N-1, h = X/(N-1)\},$$

where h is the chosen spatial step-size. The resulting semi-discrete system of ordinary differential equations has the following expression

$$u'_0(t) = u'_{N-1}(t), \quad (2.3a)$$

$$u'_i(t) = d_1 \Delta_n^{(II)}[u_i(t), h] + a_1 \Delta_n^{(I)}[u_i(t), h] + f_1(u_i(t), v_i(t)), \quad i = 1, \dots, N-2 \quad (2.3b)$$

$$v'_0(t) = v'_{N-1}(t) \quad (2.3c)$$

$$v'_i(t) = d_2 \Delta_n^{(II)}[v_i(t), h] + a_2 \Delta_n^{(I)}[v_i(t), h] + f_2(u_i(t), v_i(t)), \quad i = 1, \dots, N-2 \quad (2.3d)$$

where

$$u_i(t) = u(x_i, t), \quad v_i(t) = v(x_i, t), \quad i = 0, \dots, N-1,$$

while $\Delta_n^{(II)}[\phi_i(t), h]$ and $\Delta_n^{(I)}[\phi_i(t), h]$ (with $\phi_i(t) = u_i(t)$ or $\phi_i(t) = v_i(t)$) are the n -point fitted finite difference formulae used to approximate the second spatial derivatives and the first spatial derivatives, respectively. The system (2.3) is also joined with the initial conditions

$$u_i(0) = \psi_1(x_i), \quad v_i(0) = \psi_2(x_i), \quad i = 0, \dots, N-1. \quad (2.4)$$

For the approximation of the spatial derivatives, we follow the well-known trigonometrical fitting procedure (see, for instance, [14, 17]) which consists in constructing formulae in order to be exact on basis functions belonging to a finite-dimensional space called *fitting space*. Such functions are chosen according to the a-priori information about the qualitative behaviour of the exact solution. Since we focus on problems having periodic solutions, we choose the following trigonometric fitting space

$$\mathcal{F} = \{1, \sin(\mu x), \cos(\mu x)\}, \quad (2.5)$$

with spatial frequency $\mu \in \mathbb{R}_+$ and we adapt the three-point finite difference formulae to compute the required spatial derivatives.

As in [5, 6], we consider the three-point finite difference formula to approximate the second spatial derivative

$$\Delta_3^{(II)}[\phi_i(t), h] = \frac{1}{h^2} (a_0(z) \phi_{i-1}(t) + a_1(z) \phi_i(t) + a_2(z) \phi_{i+1}(t)), \quad (2.6)$$

and we impose its exactness (within round-off error) on functions belonging to the trigonometrical fitting space (2.5), thus obtaining the following expressions for the coefficients:

$$a_0(z) = \frac{z^2}{2(1 - \cos z)} = a_2(z), \quad a_1(z) = -\frac{z^2}{1 - \cos z}, \quad (2.7)$$

with $z = \mu h$. Such coefficients are no longer constant, as in general purpose formulae, but depend on the parameter z . In general, $z \neq 0$ because $h \neq 0$ and the frequency is not null in case of periodic solutions. Nonetheless, when z tends to 0, the variable coefficients (2.7) tend to the classical ones:

$$a_0 = 1 = a_2, \quad a_1 = -2. \quad (2.8)$$

Therefore, the trigonometrically fitted formula preserves the second order of accuracy of the corresponding classic one.

In a similar way, we develop the adapted three-point finite difference formula for the approximation of the first spatial derivative:

$$\Delta_3^{(D)}[\phi_i(t), h] = \frac{1}{h} (b_0(z) \phi_{i-1}(t) + b_1(z) \phi_i(t) + b_2(z) \phi_{i+1}(t)). \quad (2.9)$$

The linear difference operator associated to (2.9) is given by

$$\mathcal{L}[h, \underline{b}(z)]\phi(x, t) = \frac{\partial\phi(x, t)}{\partial x} - \frac{1}{h} [b_0(z) \phi(x - h, t) + b_1(z) \phi(x, t) + b_2(z) \phi(x + h, t)]. \quad (2.10)$$

Imposing the exactness of the formula (2.9) on functions belonging to the above-mentioned trigonometrical fitting space (2.5) is equivalent to annihilating the linear difference operator (2.10) on such functions. Moreover, since the difference operator is invariant for translations, it is sufficient to annihilate it for $x = 0$:

$$\begin{aligned} \mathcal{L}[h, \underline{b}(z)]1 \Big|_{x=0} &= b_0(z) + b_1(z) + b_2(z) = 0, \\ \mathcal{L}[h, \underline{b}(z)]\sin(\mu x) \Big|_{x=0} &= b_0(z) \sin z - b_2(z) \sin z + z = 0, \\ \mathcal{L}[h, \underline{b}(z)]\cos(\mu x) \Big|_{x=0} &= b_0(z) \cos z + b_1(z) + b_2(z) \cos z = 0. \end{aligned} \quad (2.11)$$

Thus, the coefficients of the trigonometrically fitted three-point formula (2.9) are

$$b_0(z) = -\frac{z}{2 \sin z}, \quad b_1(z) = 0, \quad b_2(z) = \frac{z}{2 \sin z}. \quad (2.12)$$

Also in this case, the arising coefficients, when z tends to 0, assume the classic values

$$b_0 = -\frac{1}{2}, \quad b_1 = 0, \quad b_2 = \frac{1}{2}. \quad (2.13)$$

Therefore, the trigonometrically fitted formula preserves the second order of accuracy of the corresponding classic one also in this case.

As regards time integration, we consider the equivalent formulation of the system (2.3b)-(2.3d)

$$\begin{aligned} U'(t) &= d_1 A(z)U(t) + a_1 B(z)U(t) + F_1(U(t), V(t)), \\ V'(t) &= d_2 A(z)V(t) + a_2 B(z)V(t) + F_2(U(t), V(t)), \end{aligned} \quad (2.14)$$

with

$$\begin{aligned} U(t) &= \begin{bmatrix} u_1(t) \\ u_2(t) \\ \vdots \\ u_{N-1}(t) \end{bmatrix}, & F_1(t) &= \begin{bmatrix} f_1(u_1(t), v_1(t)) \\ f_1(u_2(t), v_2(t)) \\ \vdots \\ f_1(u_{N-1}(t), v_{N-1}(t)) \end{bmatrix}, \\ V(t) &= \begin{bmatrix} v_1(t) \\ v_2(t) \\ \vdots \\ v_{N-1}(t) \end{bmatrix}, & F_2(t) &= \begin{bmatrix} f_2(u_1(t), v_1(t)) \\ f_2(u_2(t), v_2(t)) \\ \vdots \\ f_2(u_{N-1}(t), v_{N-1}(t)) \end{bmatrix}, \\ \delta_2(z) &= \frac{z^2}{2(1 - \cos z)}, & A(z) &= \frac{\delta_2(z)}{h^2} \begin{bmatrix} -2 & 1 & & 1 \\ 1 & -2 & 1 & \\ & & \ddots & \\ 1 & & & 1 & -2 \end{bmatrix}, \\ \delta_1(z) &= \frac{z}{\sin z}, & B(z) &= \frac{\delta_1(z)}{2h} \begin{bmatrix} 0 & 1 & & -1 \\ -1 & 0 & 1 & \\ & & \ddots & \\ 1 & & & -1 & 0 \end{bmatrix}, \end{aligned}$$

or, in a more compact form,

$$W'(t) = \mathcal{A}(z)W(t) + \mathcal{B}(z)W(t) + \mathcal{F}(W(t)), \quad (2.15)$$

where

$$\begin{aligned} W &= \begin{bmatrix} U \\ V \end{bmatrix}, & \mathcal{A}(z) &= \begin{bmatrix} d_1 A(z) & \\ & d_2 A(z) \end{bmatrix}, \\ \mathcal{B}(z) &= \begin{bmatrix} a_1 B(z) & \\ & a_2 B(z) \end{bmatrix}, & \mathcal{F} &= \begin{bmatrix} F_1 \\ F_2 \end{bmatrix}. \end{aligned}$$

2.1. Time integration by IMEX methods

The components of the system of ODEs (2.15) arise from different processes (diffusion, advection and reaction), so they reveal a different nature: the diffusion term is typically stiff and the reaction and advection constituents may be nonlinear [1, 12, 30].

Due to the presence of a stiff part, a totally explicit method would be stable only using a very small step-size. On the other side, an implicit method would better treat the stiffness but it would be more expensive and more complex than explicit ones, especially because of the nonlinearity. In similar cases, it may be more convenient employing the so-called implicit-explicit (IMEX) methods (see [1, 2, 3, 4, 19, 30] and references therein), which implicitly integrate only the components that need it (stiff constituents) and explicitly integrate the others, achieving benefits in stability and efficiency.

Let us now describe how a general IMEX method works. We consider the following differential problem

$$\dot{u} = f(u) + \nu g(u), \quad t \in [0, T], \quad (2.16)$$

where $f(u)$ is a possibly nonlinear term that we do not want to integrate implicitly, while $\nu g(u)$ is a stiff term requiring an implicit integration (normally, when problem (2.16) arises from a spatial semidiscretization of a reaction-diffusion PDE, $\nu g(u)$ is connected to the diffusion term). We next consider a uniform time grid of M points

$$t_j = jk, \quad j = 0, 1, \dots, M-1,$$

in $[0, T]$, with constant stepsize k . Then, general linear s -step IMEX methods are defined by [2]

$$u^{n+1} + \sum_{j=0}^{s-1} a_j u^{n-j} = k \sum_{j=0}^{s-1} b_j f(u^{n-j}) + \nu \sum_{j=-1}^{s-1} c_j g(u^{n-j}), \quad (2.17)$$

where $c_{-1} \neq 0$. One can recognize from (2.17) that, as desired, the term depending on $f(u)$ is explicitly integrated, while that depending on $g(u)$ is integrated implicitly. An example of IMEX method is given, for instance, by the so-called Euler-IMEX discretization [2], given by

$$u^{n+1} - u^n = k(f(u^n) + \nu g(u^{n+1})), \quad (2.18)$$

having order 1. Further examples of IMEX methods, also of higher order, are given in [1, 2, 19].

We now specialize the Euler-IMEX discretization (2.18) to Equation (2.15), obtaining

$$\begin{aligned} U^{j+1} &= U^j + k d_1 A^{j+1} U^{j+1} + k a_1 B^j U^j + k F_1(U^j, V^j), \\ V^{j+1} &= V^j + k d_2 A^{j+1} V^{j+1} + k a_2 B^j V^j + k F_2(U^j, V^j), \end{aligned} \quad (2.19)$$

or, in a more compact form,

$$W^{j+1} = W^j + k \mathcal{A}^{j+1} W^{j+1} + k \mathcal{B}^j W^j + k F(W^j). \quad (2.20)$$

The matrices \mathcal{A} and \mathcal{B} depend on the parameter μ , which has to be estimated. The selection technique is shown in Section 4.

3. Accuracy and stability analysis

We now present an accuracy analysis of the method (2.20), denoted as IMEX-TF in the remainder of the treatise. In particular, Theorem 3.1 shows that the order of consistency of the numerical scheme is $O(z^2) + O(k)$. This result matches the expectations since the fitted finite difference formulae used to approximate spatial derivatives have order 2 and rely on z and the IMEX-Euler method has order 1.

Theorem 3.1. *The IMEX-TF method (2.20) is consistent with the problem (1.1) and the order of consistency is $O(z^2) + O(k)$, where $z = \mu h$ as in (2.7)-(2.12) and k is the time stepsize.*

Proof. The local truncation error at the $(i, j + 1)$ -grid point is given by

$$\begin{aligned} P_{h,k}^{i,j+1}[\phi] &= \frac{\phi(x_i, t_{j+1}) - \phi(x_i, t_j)}{k} - \frac{d_\phi \delta_2(z)}{h^2} (\phi(x_{i-1}, t_{j+1}) - 2\phi(x_i, t_{j+1}) + \phi(x_{i+1}, t_{j+1})) \\ &\quad - \frac{a_\phi \delta_1(z)}{2h} (\phi(x_{i+1}, t_j) - \phi(x_{i-1}, t_j)) - f_\phi(u(x_i, t_j), v(x_i, t_j)), \end{aligned} \quad (3.1)$$

where $\phi = u$ or $\phi = v$ and

$$\begin{aligned} a_\phi &= a_1, & d_\phi &= d_1, & f_\phi &= f_1, & \text{if } \phi &= u, \\ a_\phi &= a_2, & d_\phi &= d_2, & f_\phi &= f_2, & \text{if } \phi &= v. \end{aligned}$$

We consider the following Taylor series expansions in order to appropriately rewrite the residual operator (3.1)

$$\phi(x_i, t_{j+1}) = \phi(x_i, t_j) + k \left(\frac{\partial \phi}{\partial t} \right)_{i,j} + \frac{k^2}{2} \left(\frac{\partial^2 \phi}{\partial t^2} \right)_{i,j} + O(k^3), \quad (3.2a)$$

$$\phi(x_{i+1}, t_{j+1}) = \phi(x_i, t_{j+1}) + h \left(\frac{\partial \phi}{\partial x} \right)_{i,j+1} + \frac{h^2}{2} \left(\frac{\partial^2 \phi}{\partial x^2} \right)_{i,j+1} + O(h^3), \quad (3.2b)$$

$$\phi(x_{i-1}, t_{j+1}) = \phi(x_i, t_{j+1}) - h \left(\frac{\partial \phi}{\partial x} \right)_{i,j+1} + \frac{h^2}{2} \left(\frac{\partial^2 \phi}{\partial x^2} \right)_{i,j+1} + O(h^3), \quad (3.2c)$$

$$\left(\frac{\partial^2 \phi}{\partial x^2} \right)_{i,j+1} = \left(\frac{\partial^2 \phi}{\partial x^2} \right)_{i,j} + k \left[\frac{\partial}{\partial t} \left(\frac{\partial^2 \phi}{\partial x^2} \right) \right]_{i,j} + \frac{k^2}{2} \left[\frac{\partial^2}{\partial t^2} \left(\frac{\partial^2 \phi}{\partial x^2} \right) \right]_{i,j} + O(k^3), \quad (3.2d)$$

$$\phi(x_{i+1}, t_j) = \phi(x_i, t_j) + h \left(\frac{\partial \phi}{\partial x} \right)_{i,j} + \frac{h^2}{2} \left(\frac{\partial^2 \phi}{\partial x^2} \right)_{i,j} + O(h^3), \quad (3.2e)$$

$$\phi(x_{i-1}, t_j) = \phi(x_i, t_j) - h \left(\frac{\partial \phi}{\partial x} \right)_{i,j} + \frac{h^2}{2} \left(\frac{\partial^2 \phi}{\partial x^2} \right)_{i,j} + O(h^3). \quad (3.2f)$$

We next reformulate the equation (3.2a) as follows

$$\frac{\phi(x_i, t_{j+1}) - \phi(x_i, t_j)}{k} = \left(\frac{\partial \phi}{\partial t} \right)_{i,j} + \frac{k}{2} \left(\frac{\partial^2 \phi}{\partial t^2} \right)_{i,j} + \mathcal{O}(k^2),$$

we sum (3.2b) and (3.2c), taking into account (3.2d), obtaining

$$\phi(x_{i+1}, t_{j+1}) - 2\phi(x_i, t_{j+1}) + \phi(x_{i-1}, t_{j+1}) = h^2 \left(\frac{\partial^2 \phi}{\partial x^2} \right)_{i,j} + h^2 k \left[\frac{\partial}{\partial t} \left(\frac{\partial^2 \phi}{\partial x^2} \right) \right]_{i,j} + \mathcal{O}(k^2 h^2) + \mathcal{O}(h^4),$$

and we subtract the (3.2f) from the (3.2e), achieving

$$\phi(x_{i+1}, t_j) - \phi(x_{i-1}, t_j) = 2h \left(\frac{\partial \phi}{\partial x} \right)_{i,j} + \mathcal{O}(h^3).$$

We now expand $\delta_1(z)$ and $\delta_2(z)$ in power series as follows

$$\delta_1(z) = 1 + \frac{z^2}{6} + \frac{7z^4}{360} + \mathcal{O}(z^6), \quad \delta_2(z) = 1 + \frac{z^2}{12} + \frac{z^4}{240} + \mathcal{O}(z^6).$$

Hence, the local truncation error (3.1) becomes

$$\begin{aligned} P_{h,k}^{i,j+1}[\phi] &= \left(\frac{\partial \phi}{\partial t} \right)_{i,j} + \frac{k}{2} \left(\frac{\partial^2 \phi}{\partial t^2} \right)_{i,j} + \mathcal{O}(k^2) - f_\phi(u(x_i, t_j), v(x_i, t_j)) \\ &\quad - \frac{d_\phi}{h^2} \left[1 + \frac{z^2}{12} + \frac{z^4}{240} + \mathcal{O}(z^6) \right] \left[h^2 \left(\frac{\partial^2 \phi}{\partial x^2} \right)_{i,j} + h^2 k \left(\frac{\partial}{\partial t} \left(\frac{\partial^2 \phi}{\partial x^2} \right) \right)_{i,j} + \mathcal{O}(h^2 k^2) + \mathcal{O}(h^4) \right] \\ &\quad - \frac{a_\phi}{2h} \left[1 + \frac{z^2}{6} + \frac{7z^4}{360} + \mathcal{O}(z^6) \right] \left[2h \left(\frac{\partial \phi}{\partial x} \right)_{i,j} + \mathcal{O}(h^3) \right] \\ &= \left(\frac{\partial \phi}{\partial t} \right)_{i,j} - d_\phi \left(\frac{\partial^2 \phi}{\partial x^2} \right)_{i,j} - a_\phi \left(\frac{\partial \phi}{\partial x} \right)_{i,j} - f_\phi(u(x_i, t_j), v(x_i, t_j)) \\ &\quad + k \left[\frac{1}{2} \left(\frac{\partial^2 \phi}{\partial t^2} \right)_{i,j} - d_\phi \left(\frac{\partial}{\partial t} \left(\frac{\partial^2 \phi}{\partial x^2} \right) \right)_{i,j} \right] + \mathcal{O}(k^2) + \mathcal{O}(h^2) \\ &\quad - z^2 \left[\frac{d_\phi}{12} \left(\frac{\partial^2 \phi}{\partial x^2} \right)_{i,j} + \frac{a_\phi}{6} \left(\frac{\partial \phi}{\partial x} \right)_{i,j} + \mathcal{O}(h^2) + \mathcal{O}(k) \right] + \mathcal{O}(z^4). \end{aligned}$$

Since $u(x, t)$ and $v(x, t)$ are the components of the exact solution of the problem (1.1), the following equation is verified

$$\left(\frac{\partial \phi}{\partial t} \right)_{i,j} - d_\phi \left(\frac{\partial^2 \phi}{\partial x^2} \right)_{i,j} - a_\phi \left(\frac{\partial \phi}{\partial x} \right)_{i,j} - f_\phi(u(x_i, t_j), v(x_i, t_j)) = 0.$$

Thus, the local truncation error assumes the following expression

$$\begin{aligned} P_{h,k}^{i,j+1}[\phi] &= k \left[\frac{1}{2} \left(\frac{\partial^2 \phi}{\partial t^2} \right)_{i,j} - d_\phi \left(\frac{\partial}{\partial t} \left(\frac{\partial^2 \phi}{\partial x^2} \right) \right)_{i,j} \right] + \mathcal{O}(k^2) + \mathcal{O}(h^2) \\ &\quad - z^2 \left[\frac{d_\phi}{12} \left(\frac{\partial^2 \phi}{\partial x^2} \right)_{i,j} + \frac{a_\phi}{6} \left(\frac{\partial \phi}{\partial x} \right)_{i,j} + \mathcal{O}(h^2) + \mathcal{O}(k) \right] + \mathcal{O}(z^4) \quad (3.3) \\ &= \mathcal{O}(k) + \mathcal{O}(z^2). \end{aligned}$$

□

Theorem 3.1 also allows us to prove the convergence of the numerical scheme (2.20), as explained in the following theorem.

Theorem 3.2. *Suppose that the vector valued function $F(W(\cdot, t_j))$ is smooth enough and satisfies the bound*

$$\|\nabla F\|_\infty \leq F_{max}.$$

Then, the global error

$$E^{j+1} = W(\cdot, t_{j+1}) - W^{j+1}$$

fulfills the bound

$$\|E^{j+1}\|_\infty \leq (1 + kB_{max} + kF_{max})^j \sum_{\beta=0}^j \frac{1}{(1 - kA_{max})^{\beta+1}} \max_{s=1,2,\dots,j+1} \|\mathcal{R}_{h,k}^{(s)}\|_\infty,$$

being $\mathcal{R}_{h,k}^{(j+1)} = O(k) + O(z^2)$ and A_{max} and B_{max} upper bounds for $\|\mathcal{A}(z)\|_\infty$ and $\|\mathcal{B}(z)\|_\infty$, respectively. In other terms, under the above hypothesis, the IMEX-TF method (2.20) is convergent.

Proof: The discretization error in a fixed time grid point t_{j+1} is

$$E^{j+1} = W(\cdot, t_{j+1}) - W^{j+1}, \quad (3.4)$$

where $W(\cdot, t_{j+1})$ is the exact solution in t_{j+1} . Consistency of the method (see Theorem 3.1) implies that

$$W(\cdot, t_{j+1}) = W(\cdot, t_j) + k \mathcal{A}(z) W(\cdot, t_{j+1}) + k \mathcal{B}(z) W(\cdot, t_j) + k F(W(\cdot, t_j)) + \mathcal{R}_{h,k}^{(j+1)}, \quad (3.5)$$

where $\mathcal{R}_{h,k}^{(j+1)} = O(k) + O(z^2)$.

Hence, the discretization error (3.4) becomes

$$\begin{aligned} E^{j+1} &= W(\cdot, t_j) + k \mathcal{A}(z) W(\cdot, t_{j+1}) + k \mathcal{B}(z) W(\cdot, t_j) + k F(W(\cdot, t_j)) + \mathcal{R}_{h,k}^{(j+1)} \\ &\quad - W^j - k \mathcal{A}(z) W^{j+1} - k \mathcal{B}(z) W^j - k F(W^j) \\ &= E^j + k \mathcal{A}(z) E^{j+1} + k \mathcal{B}(z) E^j + k (F(W(\cdot, t_j)) - F(W^j)) + \mathcal{R}_{h,k}^{(j+1)}. \end{aligned}$$

Since by assumption F is smooth enough, we can apply the Mean Value Theorem:

$$\|F(W(\cdot, t_j)) - F(W^j)\|_\infty = \|\nabla F\|_\infty \|W(\cdot, t_j) - W^j\|_\infty = \|\nabla F\|_\infty \|E^j\|_\infty.$$

Moreover, the hypothesis $\|\nabla F\|_\infty \leq F_{max}$ leads to

$$\|F(W(\cdot, t_j)) - F(W^j)\|_\infty \leq F_{max} \|E^j\|_\infty.$$

We next take into account the following norms

$$\begin{aligned} \|\mathcal{A}(z)\|_\infty &= d_{max} \|A(z)\|_\infty = d_{max} \frac{4\delta_2(z)}{h^2} = d_{max} \frac{2\mu^2}{1 - \cos(\mu h)} \leq A_{max}, \\ \|\mathcal{B}(z)\|_\infty &= a_{max} \|B(z)\|_\infty = a_{max} \frac{\delta_1(z)}{2h} = a_{max} \frac{\mu}{2 \sin(\mu h)} \leq B_{max}, \end{aligned}$$

being $d_{max} = \max\{d_1, d_2\}$ and $a_{max} = \max\{a_1, a_2\}$. Hence, we can obtain an upper bound for the norm of the discretization error:

$$\begin{aligned} \|E^{j+1}\|_\infty &\leq \|E^j\|_\infty + k\|\mathcal{A}(z)\|_\infty \|E^{j+1}\|_\infty + k\|\mathcal{B}(z)\|_\infty \|E^j\|_\infty \\ &\quad + k\|F(W(\cdot, t_j)) - F(W^j)\|_\infty + \|\mathcal{R}_{h,k}^{(j+1)}\|_\infty \\ &\leq \|E^j\|_\infty + kA_{max}\|E^{j+1}\|_\infty + kB_{max}\|E^j\|_\infty + kF_{max}\|E^j\|_\infty + \|\mathcal{R}_{h,k}^{(j+1)}\|_\infty. \end{aligned}$$

The last inequality can be recast by isolating the discretization error at $j + 1$ step

$$\|E^{j+1}\|_\infty \leq \frac{1 + kB_{max} + kF_{max}}{1 - kA_{max}} \|E^j\|_\infty + \frac{1}{1 - kA_{max}} \|\mathcal{R}_{h,k}^{(j+1)}\|_\infty. \quad (3.6)$$

We indicate

$$Q = \frac{1 + kB_{max} + kF_{max}}{1 - kA_{max}} \quad \text{and} \quad S = \frac{1}{1 - kA_{max}},$$

and recursively apply Equation (3.6) until the discretization error at first step appears, as follows:

$$\begin{aligned} \|E^{j+1}\|_\infty &\leq Q\|E^j\|_\infty + S\|\mathcal{R}_{h,k}^{(j+1)}\|_\infty \\ &\leq Q^{j+1}\|E^0\|_\infty + Q^j S\|\mathcal{R}_{h,k}^{(1)}\|_\infty + \dots + QS\|\mathcal{R}_{h,k}^{(j)}\|_\infty + S\|\mathcal{R}_{h,k}^{(j+1)}\|_\infty. \end{aligned}$$

Since $\|E^0\|_\infty = 0$, the following inequality holds for each j :

$$\begin{aligned} \|E^{j+1}\|_\infty &\leq S(Q^j + Q^{j-1} + \dots + Q + 1) \max_{s=1,2,\dots,j+1} \|\mathcal{R}_{h,k}^{(s)}\|_\infty \\ &\leq (1 + kB_{max} + kF_{max})^j \sum_{\beta=0}^j \frac{1}{(1 - kA_{max})^{\beta+1}} \max_{s=1,2,\dots,j+1} \|\mathcal{R}_{h,k}^{(s)}\|_\infty \xrightarrow{h,k \rightarrow 0} 0. \end{aligned}$$

□

Finally, we provide the following stability analysis of the numerical scheme (2.20).

Theorem 3.3. *Suppose that the vector valued function $F(W(\cdot, t_j))$ is smooth enough and satisfies the bound*

$$\|\nabla F\|_\infty \leq F_{max}. \quad (3.7)$$

If

$$\|(\mathbb{I} - k\mathcal{A})^{-1}\|_\infty \left(\|\mathbb{I} + k\mathcal{B}(z)\|_\infty + kF_{max} \right) \leq 1, \quad (3.8)$$

then the method (2.20) is stable.

Proof: Following the idea in [29], a method is stable if the error caused by an incoming perturbation does not blow up. For this reason, we perturb the solution W^j as follows

$$\widetilde{W}^j = W^j + \delta,$$

and we write the numerical scheme (2.20) for both W^j and \tilde{W}^j :

$$W^{j+1} = (\mathbb{I} - k\mathcal{A}(z))^{-1} (\mathbb{I} + k\mathcal{B}(z)) W^j + k(\mathbb{I} - k\mathcal{A}(z))^{-1} F(W^j), \quad (3.9a)$$

$$\tilde{W}^{j+1} = (\mathbb{I} - k\mathcal{A}(z))^{-1} (\mathbb{I} + k\mathcal{B}(z)) \tilde{W}^j + k(\mathbb{I} - k\mathcal{A}(z))^{-1} F(\tilde{W}^j). \quad (3.9b)$$

The error $E^{j+1} = W^{j+1} - \tilde{W}^{j+1}$ due to the perturbation is given by

$$E^{j+1} = (\mathbb{I} - k\mathcal{A}(z))^{-1} (\mathbb{I} + k\mathcal{B}(z)) E^j + k(\mathbb{I} - k\mathcal{A}(z))^{-1} (F(W^j) - F(\tilde{W}^j)),$$

and its norm verifies the following inequality

$$\|E^{j+1}\|_\infty \leq \vartheta \|\mathbb{I} + k\mathcal{B}(z)\|_\infty \|E^j\|_\infty + k\vartheta \|F(W^j) - F(\tilde{W}^j)\|_\infty,$$

where $\vartheta = \|(\mathbb{I} - k\mathcal{A}(z))^{-1}\|_\infty$. Applying the Mean Value Theorem to the reaction term and exploiting the hypothesis (3.7), we derive the following bound

$$\|F(W^j) - F(\tilde{W}^j)\|_\infty \leq \|\nabla F\|_\infty \|W^j - \tilde{W}^j\|_\infty \leq F_{max} \|E^j\|_\infty, \quad (3.10)$$

which leads to

$$\|E^{j+1}\|_\infty \leq \vartheta (\|\mathbb{I} + k\mathcal{B}(z)\|_\infty + kF_{max}) \|E^j\|_\infty.$$

This stability inequality implies the stability condition

$$\vartheta (\|\mathbb{I} + k\mathcal{B}(z)\|_\infty + kF_{max}) \leq 1,$$

that gives the thesis. □

4. Parameter selection

We now propose a strategy to estimate the parameter μ in (2.5), necessary for the computation of the coefficients (2.7) and (2.12) of the trigonometrically fitted finite difference formulae for the approximation of the spatial derivatives. The proposed strategy relies on manipulating the leading term of the local truncation error, whose expression at each grid point is provided in the proof of the Theorem 3.1, i.e.

$$\begin{aligned} P_{h,k}^{i,j+1}[\phi] &= k \left[\frac{1}{2} \left(\frac{\partial^2 \phi}{\partial t^2} \right)_{i,j} - d_\phi \left(\frac{\partial}{\partial t} \left(\frac{\partial^2 \phi}{\partial x^2} \right) \right)_{i,j} \right] + \mathcal{O}(k^2) + \mathcal{O}(h^2) \\ &\quad - z^2 \left[\frac{d_\phi}{12} \left(\frac{\partial^2 \phi}{\partial x^2} \right)_{i,j} + \frac{a_\phi}{6} \left(\frac{\partial \phi}{\partial x} \right)_{i,j} + \mathcal{O}(h^2) + \mathcal{O}(k) \right] + \mathcal{O}(z^4), \end{aligned}$$

where $\phi = u$ or $\phi = v$ and $z = \mu h$. Its z -dependent part in the leading term is given by

$$T^{i,j+1}(z) = -\frac{z^2}{6} \left[\frac{d_\phi}{2} \left(\frac{\partial^2 \phi}{\partial x^2} \right)_{i,j} + a_\phi \left(\frac{\partial \phi}{\partial x} \right)_{i,j} \right]. \quad (4.1)$$

We first manipulate the expression (4.1), by approximating the involved spatial derivatives through the trigonometrically fitted finite difference formula (2.6) and (2.9) with coefficients (2.7) and (2.12), obtaining

$$T^{i,j+1}(z) \approx \bar{T}^{i,j+1}(z) = -\frac{z^2}{6} \left(\frac{d_\phi \alpha_{i,j}}{4h^2} \frac{z^2}{1 - \cos z} + a_\phi \beta_{i,j} \frac{z}{2h \sin z} \right), \quad (4.2)$$

and we estimate the parameter μ at each inner grid point with a value that annihilates the function (4.2). Since $z > 0$, we solve the nonlinear system

$$d_\phi \alpha_{i,j} z \sin z + 2ha_\phi \beta_{i,j}(1 - \cos z) = 0.$$

For this purpose, we consider the Mc-Laurin expansion of the functions $\sin z$ and $1 - \cos z$ truncated at the fourth order term and solve the nonlinear algebraic equation

$$d_\phi \alpha_{i,j} \left(1 - \frac{z^2}{6}\right) + h a_\phi \beta_{i,j} \left(1 - \frac{z^2}{12}\right) = 0,$$

whose solutions are

$$z = \pm \sqrt{\frac{12(d_\phi \alpha_{i,j} + h a_\phi \beta_{i,j})}{(2d_\phi \alpha_{i,j} + h a_\phi \beta_{i,j})}}.$$

Therefore, an estimate for the parameter μ is the following

$$\mu = \frac{1}{h} \sqrt{\frac{12(d_\phi |\alpha_{i,j}| + h a_\phi |\beta_{i,j}|)}{(2d_\phi |\alpha_{i,j}| + h a_\phi |\beta_{i,j}|)}}. \quad (4.3)$$

This result can be improved by considering a control factor $\zeta < 1$ which depends on the problem and satisfies

$$C_{i,j} \zeta^2 \leq 1, \quad (4.4)$$

where

$$C_{i,j} = \left| \frac{24(d_\phi \alpha_{i,j} + h a_\phi \beta_{i,j})}{2d_\phi \alpha_{i,j} + h a_\phi \beta_{i,j}} \right|. \quad (4.5)$$

Indeed, the following relation holds:

$$|T^{i,j+1}(\zeta\mu)| = \frac{h^2}{12} \zeta^2 C_{i,j} D_{i,j} \leq \frac{h^2}{12} D_{i,j} \leq \frac{h^2}{12} C_{i,j} D_{i,j} = |T^{i,j+1}(\mu)|, \quad (4.6)$$

where $T^{i,j+1}$ is the leading term of the local truncation error given by (4.1) and

$$D_{i,j} = \left| \frac{d_\phi}{2} \left(\frac{\partial^2 \phi}{\partial x^2} \right)_{i,j} + a_\phi \left(\frac{\partial \phi}{\partial x} \right)_{i,j} \right|. \quad (4.7)$$

We observe that the last inequality in (4.6) derives from $C_{i,j} \geq 1$. The relation (4.6) shows that $|T^{i,j+1}(\zeta\mu)|$ is closer to the minimum of $T^{i,j+1}$ than $|T^{i,j+1}(\mu)|$, so the control

factor ζ improves the estimate of the parameter μ . Hence, we compute this factor by using the condition (4.4)

$$\zeta = \sqrt{\frac{2d_\phi + ha_\phi}{24(d_\phi + ha_\phi)}} \quad (4.8)$$

and we estimate the parameter μ as follows

$$\bar{\mu} = \frac{\zeta}{h} \sqrt{\frac{12(d_\phi |\alpha_{i,j}| + h a_\phi |\beta_{i,j}|)}{(2d_\phi |\alpha_{i,j}| + h a_\phi |\beta_{i,j}|)}}. \quad (4.9)$$

We observe that the estimate (4.9) does not require a larger additional computational effort, such as in [7, 8, 9, 11] and references therein, because it does not rely on employing numerical solvers for algebraic equations or numerical optimization strategies.

5. Numerical experiments

We now provide some numerical results concerning the integration of some advection-reaction-diffusion problems. In the remainder of this section, we refer to the introduced scheme (2.20) as IMEX-TF and to the classic forward-backward Euler method applied to the system (2.15) as IMEX-class.

Example 5.1. We consider the following system

$$\begin{aligned} \frac{\partial u}{\partial t} &= d_1 \frac{\partial^2 u}{\partial x^2} + a_1 \frac{\partial u}{\partial x} + (a_1 - d_1) t + d_1 u - a_1 v + (u - v)^2 + \sin(2x), \\ \frac{\partial v}{\partial t} &= d_2 \frac{\partial^2 v}{\partial x^2} + a_2 \frac{\partial v}{\partial x} - (a_2 + d_2) t + a_2 u + d_2 v + u^2 + v^2 - 2t(u + v) + 2t^2, \end{aligned} \quad (5.1)$$

where $u, v : \mathcal{D} = [0, 4\pi] \times [0, 1] \rightarrow \mathbb{R}$, $d_1 = 0.5$, $d_2 = 0.1$, $a_1 = 0.5$, $a_2 = 0.1$. This problem is equipped by initial conditions

$$u(x, 0) = \sin x, \quad v(x, 0) = \cos x, \quad x \in [0, 4\pi], \quad (5.2)$$

and periodic boundary conditions

$$u(0, t) = t = u(4\pi, t), \quad v(0, t) = t + 1 = v(4\pi, t), \quad t \in [0, 1]. \quad (5.3)$$

The exact solution is given by

$$u = t + \sin x, \quad v = t + \cos x,$$

and, therefore, it lies in the functional space spanned by (2.5). For this reason, the adoption of the trigonometrically fitted method (2.20) is justified and the exact value for the parameter μ on which the basis functions (2.5) depend is equal to the exact frequency in the spatial oscillations, i.e. $\mu = 1$.

As shown in Figure 1, the numerical solution of the problem (5.1) computed by the numerical method (2.20) oscillates in space with constant shape and speed and matches well the periodic boundary conditions. Moreover, Table 1 shows that, using the same spatial integration stepsize, the IMEX-TF method (2.20) is much more accurate than its classic counterpart IMEX-class, based on algebraic polynomials. Actually, the classic method achieves the same accuracy obtained by the IMEX-TF with $\bar{h} = \pi/5$ when the spatial integration stepsize is reduced to $h = \bar{h}/64$ at least. This extreme reduction strongly increases the computational cost, so the IMEX-TF scheme appears much more convenient.

It is definitely important to stress that this good property of the method (2.20) IMEX-TF is influenced by the knowledge of an accurate value of the parameter μ , as it is evident in Table 2. Indeed, the error drastically increases when the value of the parameter μ moves away from the exact value $\mu = 1$ and becomes almost the same obtained by the classic IMEX when $\mu = 0.2$. In this case, it is more convenient using the IMEX-class method because it is much more efficient. Therefore, when the exact values of the parameters correlated to trigonometrical fitting are unknown, the significant benefits of this strategy could be lost unless an accurate technique is employed to estimate them. Following the idea presented in Section 4, we estimate the parameter μ at each grid point by minimizing the μ -dependent leading term of the local truncation error. Although the exact spatial frequency is constant, its estimate is pointwise computed in order to limit the accumulation of the error. Table 3 shows that the IMEX-TF method combined with this estimate is still more accurate than the corresponding classic one. Finally, Figure 2 depicts the estimate for the parameter μ at each grid point. We highlight that the estimated values for the parameter are significantly close to the exact value ($\mu = 1$).

Method	h	CPU Time	Error
IMEX-TF	$\pi/5$	114.551534	0.000006
IMEX-class	$\pi/5$	7.254047	0.103574
IMEX-class	$\pi/10$	78.499703	0.025453
IMEX-class	$\pi/20$	29.452989	0.006355
IMEX-class	$\pi/40$	132.944052	0.001592
IMEX-class	$\pi/80$	1627.527233	0.000398
IMEX-class	$\pi/160$	14774.495908	0.000099

Table 1: Comparison between the IMEX-TF method (2.20) and the corresponding classic IMEX in terms of spent time and true error for the integration of (5.1) joined with initial conditions (5.2) and periodic boundary conditions (5.3). The IMEX-TF method has been applied using the exact value for the spatial frequency ($\mu = 1$). The time stepsize is $k = 0.01$.

Example 5.2. We now integrate the following system having time-dependent model

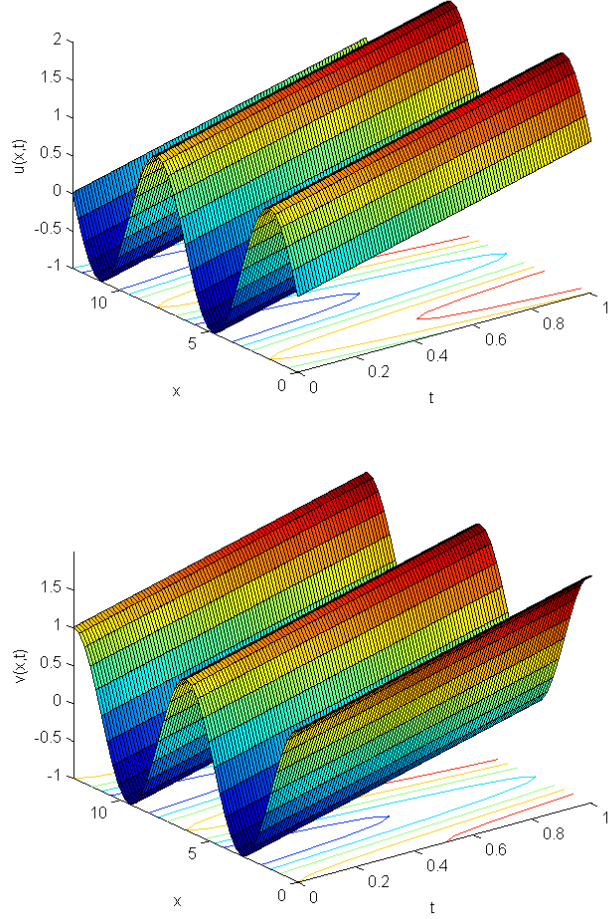


Figure 1: Numerical solution of the test problem (5.1), with initial conditions (5.2) and boundary conditions (5.3) computed by the new method (2.20) with spatial stepsize $h = \pi/10$ and time stepsize $k = 0.01$. The component $u(x, t)$ is depicted on the top and the component $v(x, t)$ is represented on the bottom.

parameters and a nonlinear reaction term:

$$\begin{aligned} \frac{\partial u}{\partial t} &= \frac{t}{2} \frac{\partial^2 u}{\partial x^2} - t \frac{\partial u}{\partial x} + u^2 + v^2 - 2t^2, \\ \frac{\partial v}{\partial t} &= \frac{t}{4} \frac{\partial^2 v}{\partial x^2} + \frac{t}{2} \frac{\partial v}{\partial x} + uv - t^2 - \frac{\sin(4x)}{2} + 1, \end{aligned} \tag{5.4}$$

where $u, v : \mathcal{D} = [0, 4\pi] \times [0, 1] \longrightarrow \mathbb{R}$. Such a problem is provided with the following

Method	μ	CPU Time	Error
IMEX-TF	1	411.717839	$2.63 \cdot 10^{-8}$
IMEX-TF	0.8	150.275763	0.009196
IMEX-TF	0.2	151.695372	0.024440
IMEX-TF	5	166.281466	0.686977
IMEX-TF	10	147.545746	2.253046
IMEX-class	–	78.499703	0.025453

Table 2: Accuracy and efficiency of the IMEX-class method and the IMEX-TF scheme (2.20) applied with different values of the parameter μ in the integration of the problem (5.1) with a time stepsize $k = 0.01$ and a spatial grid width $h = \pi/10$.

Method	μ	CPU Time	Error
IMEX-TF	1	114.551534	0.000006
IMEX-TF	Estimated	170.041090	0.038655
IMEX-class	–	7.254047	0.103574

Table 3: Accuracy and efficiency of the IMEX-class method, the IMEX-TF scheme (2.20) applied with the exact value of the parameter ($\mu = 1$) and the IMEX-TF scheme combined with the estimated value (4.9) of the parameter μ for the integration of the problem (5.1) provided with initial conditions (5.2) and periodic boundary conditions (5.3). The spatial grid width is $h = \pi/5$ and the time stepsize is $k = 0.01$.

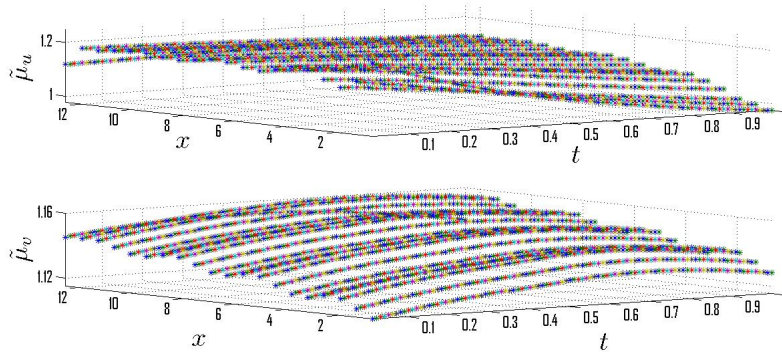


Figure 2: Estimate of the parameter in each grid point computed by using the optimization strategy described in Section 4 for the integration of test problem (5.1), with initial conditions (5.2) and boundary conditions (5.3), spatial stepsize $h = \pi/5$ and time stepsize $k = 0.01$.

initial conditions

$$u(x, 0) = -\sin 2x, \quad v(x, 0) = -\cos 2x, \quad x \in [0, 4\pi], \quad (5.5)$$

and periodic boundary condition

$$u(0, t) = t = u(4\pi, t), \quad v(0, t) = t - 1 = v(4\pi, t), \quad t \in [0, 1]. \quad (5.6)$$

Since the exact solution is

$$u = t - \sin 2x, \quad v = t - \cos 2x,$$

it could be more convenient using the trigonometrically fitted IMEX-TF scheme (2.20). In this case, the exact value of the parameter which the basis functions (2.5) depend on is $\mu = 2$.

Table 4 reports that the IMEX-TF method (2.20) applied with the exact value for the parameter μ is much more accurate than the corresponding classic IMEX Euler method. When the IMEX-TF scheme is combined with the estimated value (4.9) for this parameter, however, the accuracy decreases but it is still higher than in the classic case, as shown in Table 5.

Method	h	CPU Time	Error
IMEX-TF	$\pi/5$	28.688584	0.073308
IMEX-class	$\pi/5$	7.098046	0.925135
IMEX-class	$\pi/10$	11.372473	0.141530
IMEX-class	$\pi/20$	28.251781	0.046213

Table 4: Comparison between the IMEX-TF method (2.20) and the corresponding classic IMEX in terms of spent time and error for the integration of system (5.4) subject to initial conditions (5.5) and periodic boundary conditions (5.6). The IMEX-TF method has been applied using the exact value for the spatial frequency ($\mu = 2$). The time stepsize is $k = 0.01$.

Method	μ	CPU Time	True Error
IMEX-TF	2	28.688584	0.073308
IMEX-TF	Estimated	192.364833	0.148646
IMEX-class	–	7.098046	0.925135

Table 5: Accuracy and efficiency of the IMEX-class method, the IMEX-TF scheme (2.20) applied with the exact value for the parameter μ ($\mu = 2$) and the IMEX-TF scheme combined with the estimated value (4.9) of the parameter μ in the integration of problem (5.4) equipped by initial conditions (5.5) and periodic boundary conditions (5.6). The time stepsize is $k = 0.01$ and the spatial grid width is $h = \pi/5$.

We observe that the periodic character of the solution is independent on the periodic boundary conditions: indeed, many significant examples in the literature, also regarding applications to Mathematical Biology and relying on (advection-)reaction-diffusion problems, produce periodic wavefronts, even starting from non-periodic boundary conditions [6, 10, 12, 15, 22, 23, 24, 25, 26, 27, 28]. As an example of this feature, we provide the following numerical test.

Example 5.3. We consider the following advection-reaction-diffusion system provided with a nonlinear reaction term

$$\begin{aligned}\frac{\partial u}{\partial t} &= d_1 \frac{\partial^2 u}{\partial x^2} + a_1 \frac{\partial u}{\partial x} + (a_1 - d_1)t + d_1 u - a_1 v + (u - v)^2 + \sin 2x, \\ \frac{\partial v}{\partial t} &= d_2 \frac{\partial^2 v}{\partial x^2} + a_2 \frac{\partial v}{\partial x} - (d_2 + a_2)t + d_2 v + a_2 u + u^2 + v^2 - 2t(u + v) + 2t^2,\end{aligned}\tag{5.7}$$

where $u, v : \mathcal{D} = \left[0, \frac{5}{2}\pi\right] \times [0, 1] \longrightarrow \mathbb{R}$ and $d_1 = 0.5$, $d_2 = 0.1$, $a_1 = 0.5$ and $a_2 = 0.1$. This problem is joined with the following initial conditions

$$u(x, 0) = \sin x, \quad v(x, 0) = \cos x, \quad x \in \left[0, \frac{5}{2}\pi\right],\tag{5.8}$$

and Dirichlet boundary conditions

$$u(0, t) = t, \quad u\left(\frac{5}{2}, t\right) = t + 1, \quad v(0, t) = t + 1, \quad v\left(\frac{5}{2}, t\right) = t \quad t \in [0, 1].\tag{5.9}$$

The exact solution is given by

$$u = t + \sin x, \quad v = t + \cos x,$$

so it lies in the functional space spanned by (2.5). Hence, we properly employ the trigonometrically fitted method (2.20). The exact value for the parameter μ on which the basis functions (2.5) depend is equal to the exact frequency in the spatial oscillations, i.e. $\mu = 1$.

Also in case of Dirichlet boundary conditions, the IMEX-TF scheme exhibits higher accuracy than the corresponding IMEX-class method, even in case of estimated parameter, as reported in Tables 6 and 7.

Method	h	CPU Time	Error
IMEX-TF	$\pi/4$	21.996141	0.009786
IMEX-class	$\pi/4$	5.194833	0.151768
IMEX-class	$\pi/8$	7.815650	0.039661
IMEX-class	$\pi/16$	13.462886	0.016891
IMEX-class	$\pi/32$	31.839804	0.017157
IMEX-class	$\pi/64$	167.576274	0.017672

Table 6: Accuracy and efficiency of the IMEX-class method and the IMEX-TF scheme (2.20) applied with the exact value of the parameter ($\mu = 1$) in the integration of problem (5.7) equipped by initial conditions (5.8) and Dirichlet boundary conditions (5.9). The time stepsize is $k = 0.01$.

Method	μ	CPU Time	Error
IMEX-TF	1	21.996141	0.009786
IMEX-class	–	5.194833	0.151768
IMEX-TF	Estimated	47.486704	0.014169

Table 7: Accuracy and efficiency of the IMEX-class method, the IMEX-TF scheme (2.20) applied with the exact value of the parameter ($\mu = 1$) and the IMEX-TF scheme joined with the estimated parameter (4.9) for the integration of the problem (5.7) provided with initial conditions (5.8) and Dirichlet boundary conditions (5.9). The time stepsize is $k = 0.01$ and the spatial grid width is $h = \pi/5$.

6. Conclusions

We have developed an adapted numerical scheme to integrate advection-reaction-diffusion problems generating periodic wavefronts. In particular, we have employed trigonometrically fitted finite differences for the spatial discretization in order to accurately follow the prescribed oscillations of the exact solution more efficiently. For the time integration, we have applied an IMEX method, based on the first order forward-backward Euler method, in order to treat in an efficient way the stiff and nonstiff parts. The rigorous analysis of the good properties of the method has provided an expression of the local truncation error which leads us to estimate the parameter correlated to the coefficients of the trigonometrically fitted method without significantly increasing the overall computational cost. Numerical experiments have confirmed the effectiveness of the approach and its relation with the knowledge of an accurate estimation of the parameter.

It is worth observing that this paper is a stepping stone in the direction of applying the idea of an adapted numerical integration of multidimensional problems generating complex qualitative behaviours. For such problems, the parameters of adapted methods have to accurately be estimated along each spatial direction: this issue will be handled in future works on the topic.

Acknowledgments

This work is supported by GNCS-INDAM project. The authors are grateful to the anonymous reviewers for their precious suggestions, which helped improving the treatise.

References

- [1] Ascher, U.M., Ruuth, S.J., Spiteri, R.J., Implicit-Explicit Runge-Kutta Methods for Time-Dependent Partial Differential Equations, *Appl. Numer. Math.* 25(2-3), 151–167 (1997).
- [2] Ascher, U.M., Ruuth, S.J., Wetton, B.T.R., Implicit-Explicit methods for time-dependent partial differential equations, *SIAM J. Numer. Anal.* 32, 797–823 (1995).

- [3] Boscarino, S., Error analysis of IMEX Runge-Kutta methods derived from differential-algebraic systems, *SIAM J. Numer. Anal.* 45(4), 1600–1621 (2007).
- [4] Boscarino, S., On an accurate third order implicit-explicit Runge-Kutta method for stiff problems, *Appl. Numer. Math.* 59(7), 1515–1528 (2009).
- [5] D’Ambrosio, R., Paternoster, B., Numerical solution of a diffusion problem by exponentially fitted finite difference methods, *SpringerPlus* 3:425 (2014).
- [6] D’Ambrosio, R., Paternoster, B., Numerical solution of reaction-diffusion systems of λ - ω type by trigonometrically fitted methods, *J. Comput. Appl. Math.* (2015).
- [7] D’Ambrosio, R., Esposito, E., Paternoster, P., Exponentially fitted two-step Runge-Kutta methods: Construction and parameter selection. *Appl. Math. Comp.* 218 (14), 7468–7480 (2012).
- [8] D’Ambrosio, R., Esposito, E., Paternoster, B., Parameter estimation in exponentially fitted hybrid methods for second order ordinary differential problems. *J. Math. Chem.* 50, 155-168 (2012).
- [9] D’Ambrosio, R., Esposito, E., Paternoster, B., Exponentially fitted two-step hybrid methods for $y'' = f(x, y)$, *J. Comput. Appl. Math.* 235(16), 4888–4897 (2011).
- [10] Dunbar, S.R., Travelling wave solutions of diffusive Lotka-Volterra equations, *J. Math. Biol.* 17(1), 11–32 (1983).
- [11] Hollevoet, D., Van Daele, M., Vanden Berghe, G., Exponentially-fitted methods applied to fourth order boundary value problems, *J. Comput. Appl. Math.* 235(18), 5380–5393 (2011).
- [12] Hundsdorfer, W., Verwer, J.G., Numerical Solution of Time-Dependent Advection-Diffusion-Reaction Equations, Springer Series in Comput. Math. 33, Springer (2003).
- [13] Isaacson, E., Keller, H.B., Analysis of Numerical Methods, Dover Publications, New York (1994).
- [14] Ixaru, L.Gr., Vanden Berghe, G., Exponential Fitting, Kluwer, Boston-Dordrecht-London (2004).
- [15] Kopell, N., Howard, L.N., Plane waves solutions to reaction-diffusion equations, *Studies in Applied Mathematics* 52, 291–328 (1973).
- [16] McRea, G.J., Goodin, W.R., Seinfeld, J.H., Numerical solution of atmospheric diffusion for chemically reacting flows, *J. Comput. Phys.* 77, 1–42 (1982).
- [17] Paternoster, B., Present state-of-the-art in exponential fitting. A contribution dedicated to Liviu Ixaru on his 70-th anniversary, *Comput. Phys. Commun.* 183, 2499–2512 (2012).

- [18] Perumpanani, A. J., Sherratt, J. A., Maini, P. K., Phase differences in reaction-diffusion-advection systems and applications to morphogenesis, *J. Appl. Math.* 55, 19–33 (1995).
- [19] Ruuth, S., Implicit-explicit methods for reaction-diffusion problems in pattern formation, *J. Math. Biol.* 34, 148–176 (1995).
- [20] Schiesser, W.E., *The Numerical Method of Lines: Integration of Partial Differential Equations*, Academic Press, San Diego (1991).
- [21] Schiesser, W.E., Griffiths, G.W., *A Compendium of Partial Differential Equation Models: Method of Lines Analysis with Matlab*, Cambridge University Press (2009).
- [22] Sherratt, J.A., Periodic waves in reaction-diffusion models of oscillatory biological systems, *FORMA* 11, 61–80 (1996).
- [23] Sherratt, J.A., On the evolution of periodic plane waves in reaction-diffusion systems of λ - ω type, *SIAM J. Appl. Math.* 54, 1374–1385 (1994).
- [24] Sherratt, J.A., Smith, M.J., Transition to spatiotemporal chaos via stationary branching shocks and holes, *Physica D: Nonlinear Phenomena* 241(15), 1671–1679 (2012).
- [25] Sherratt, J.A., Smith, M.J., Periodic travelling waves in cyclic populations: field studies and reaction-diffusion models, *J. Roy. Soc. Interface* 5, 483–505 (2008).
- [26] Smith, M.J., Rademacher, J.D.M., Sherratt, J.A., Absolute stability of wavetrains can explain spatiotemporal dynamics in reaction-diffusion systems of lambda-omega type, *SIAM J. Appl. Dyn. Systems* 8, 1136–1159 (2009).
- [27] Smith, M.J., Sherratt, J.A., Lambin, X., The effects of density-dependent dispersal on the spatiotemporal dynamics of cyclic populations, *J. Theor. Biol.* 254(2), 264–274 (2008).
- [28] Smith, M.J., Sherratt, J.A., The effects of unequal diffusion coefficients on periodic travelling waves in oscillatory reaction-diffusion systems, *Physica D: Nonlinear Phenomena* 236(2), 90–103 (2007).
- [29] Smith, G.D., *Numerical solution of partial differential equations - Finite difference methods*, Clarendon Press, Oxford (1985).
- [30] Wang, H., Shu, C.W., Zhang, Q., Stability and Error Estimates of Local Discontinuous Galerkin Methods with Implicit-Explicit Time-Marching for Advection-Diffusion Problems, *SIAM J. Numer. Anal.* 53(1), 206227 (2015).